

Gallium-doped Tin Oxide Nano-cuboids for Improved Dye Sensitized Solar Cell

Jun Jie Teh^{a,b}, Siong Luong Ting^{a,b}, Kam Chew Leong^b, Jun Li^c, Peng Chen^{a},*

^aSchool of Chemical and Biomedical Engineering, Nanyang Technological University, 70 Nanyang Drive, Singapore 637457, Singapore.

^bGlobalFoundries Singapore, 60 Woodlands Industrial Park D Street 2, Singapore 738406, Singapore

^cInstitute of Materials Research and Engineering, A*STAR (Agency for Science, Technology and Research), 3 Research Link, Singapore 117602, Singapore

ABSTRACT

Tin dioxide (SnO_2) is a potential candidate to replace conventional titanium dioxide (TiO_2) in dye-sensitized solar cells (DSSCs) because of its wider bandgap and higher electron mobility. However, SnO_2 suffers from low band edge that causes severe backflow of electrons towards electrolyte (charge recombination). Herein, we demonstrate that gallium (Ga) doping can increase the band edge of SnO_2 . And we show that DSSCs using a Ga-doped SnO_2 nano-

cuboids based photoanode offer improved open circuit potential (~0.74 V), fill factor (~73.7%), and power conversion efficiency (~4.05%).

KEYWORDS: Dye Sensitized Solar Cell, Tin Oxide, Gallium Doping, Nano-cuboid, Band edge, Charge recombination

INTRODUCTION

Dye-sensitized solar cells (DSSCs) are promising green energy devices with low-cost which typically consist of a photoanode made by coating mesoporous metal-oxide semiconductor film on fluorine-doped tin oxide (FTO) glass, a platinum coated FTO counter electrode, dye molecules incorporated onto photoanode, and electrolyte.¹⁻³ But the practical use of current DSSCs is limited by their low power conversion efficiency.

The semiconducting metal-oxide material used is the key component governing the device performance, including photoelectron injection, electron transfer and transport, dye loading capacity, and charge recombination.^{4, 5} Thus far, titanium oxide (TiO₂) is the most popular choice. The conversion efficiency of TiO₂ based DSSCs, however, is largely limited by its low conductivity which, in turn, leads to undesired charge recombination. Tin oxide (SnO₂) has recently been considered as a promising alternative due to its wider bandgap (3.5 eV) which benefits for the long-term stability of DSSCs against UV degradation, and high electron mobility (~100-200 cm² V⁻¹s⁻¹) which reduces charge recombination between injected electrons and holes in valence band.^{6, 7} In addition, SnO₂ is able to form homo-junction with FTO substrate, therefore, negate the issue of high contact resistance originated from the hetero-junction between TiO₂ and FTO.⁸

But SnO₂-based DSSCs critically suffer from the problem of low conduction band edge (E_c is ~0.3 eV lower than that of anatase TiO₂), which causes fast backflow of photoelectrons to the electrolyte (a form of charge recombination) and thus reduction of open circuit voltage (V_{oc}).⁹⁻¹³ To tackle this issue, a thin layer of metal oxide with higher conduction band edge (e.g., Al₂O₃, Cr₂O₃, TiO₂, CdO, CuO, ZnO, MgO) has been coated onto SnO₂.¹⁴⁻¹⁹ Alternatively, ternary oxides (Zn₂SnO₄ and BaSnO₂) have been synthesized to favorably shift the band structure.²⁰⁻²⁵ However, the achieved improvement is still limited.

Herein we report the synthesis of gallium (Ga) doped SnO₂ nano-cuboids (Ga-SnO₂-NC) using the commercially available SnO₂ nanoparticles (SnO₂-NP) as the growth seeds under hydrothermal condition. We demonstrate that Ga-doping increases the band edge of SnO₂ whereby suppressing photoelectron backflow thus achieving a higher open circuit voltage (V_{oc} ~ 0.74 V). This value is comparable to that of TiO₂-NP based photoanodes and, to the best of our knowledge, the highest for SnO₂ based electrodes without TiO₂ coating. With a high V_{oc} as well as a high fill factor (FF ~ 73.7%), the DSSCs equipped with Ga-SnO₂-NC photoanode are able to achieve a power conversion efficiency up to ~4.05% (~185% improvement as compared to the use of commercial SnO₂ nanoparticles). Finally, the underlying mechanism of such enhancement is proposed.

2. EXPERIMENTAL SECTION

All chemicals were purchased from Sigma-Aldrich except gallium nitrate hydrate from Alfa Aesar and absolute ethanol from Merck.

2.1 SYNTHESIS OF Ga-SnO₂-NC

Ga-SnO₂-NCs were synthesized by a hydrothermal method. Specifically, 1 mmol of tin (IV) chloride pentahydrate, predetermined gallium nitrate hydrate (0, 1, 3, 5% molar ratio to tin chloride) and 15 mmol of sodium hydroxide were dissolved in 25ml DI water. After continuous stirring for 10 min, 60 mg of tin oxide nanoparticles was added and tip-sonicated for 50 cycles (2s sonication and 2s pause for each cycle). The suspension was then transferred into 40 ml Teflon-lined autoclave and reacted hydrothermally at 180°C for 24 hr. After cooling down to the room temperature, the products were centrifuged, rinsed thoroughly with distilled water for several times, and finally dried at 70 °C.

2.2 ELECTRODE FABRICATION

Ga-SnO₂-NC powder was made into paste using the standard procedure for DSSC electrode fabrication.²⁶ The photoanode was fabricated by doctor-blading the paste on fluorine-doped SnO₂ glass (FTO), with an active area of ~0.12 cm² and thickness of ~8µm. It was subsequently sintered at 450 °C for 30 min in air. Finally, the photoanode was soaked in a mixture solution of equal amount of tert-butanol and acetonitrile containing 0.475 mM N719 dye and 0.025 mM D149 dye for 16 hr at room temperature, followed by washing with ethanol. Platinum sputtered FTO was used as the counter electrode. 50 mM tri-iodide in acetonitrile (AN-50, Solaronix) was used as the low viscosity electrolyte.

2.3. CHARACTERIZATION

The crystallinity of the nanostructures was investigated using Siemens D5008 X-ray diffractometer with Cu K_α radiation ($\lambda=1.5406 \text{ \AA}$) at 40 kV and 40 mA, scanning from $2\theta= 20^\circ$ to 70° with a scan rate of 2° per minute. The morphology was observed using field emission

scanning electron microscopy (FESEM, JEOL JSM-6700) and transmission electron microscope (TEM, JEOL 2010). UV-vis absorbance spectra were measured by Shimadzu 3600 UV-vis Spectrophotometers. X-ray photoelectron spectroscopy (XPS) measurement was obtained from a ESCALAB MK-II system. The current-voltage tests of DSSCs were performed under one sun condition using a solar light simulator (Abet Technologies S2000 with 550W xenon lamp and an AM 1.5 filter, 100 mW/cm²). The dye loading capability was determined by desorbing the dye into 50% ethanol solution containing 20 mM NaOH and subsequent the UV-vis absorption measurement at 500 nm. Electrochemical impedance spectroscopy (EIS) was performed under illumination of a solar light simulator and the cell was biased at the V_{OC} induced by the illumination with the frequency range of 0.1 Hz to 0.1 MHz. The flat-band potential (V_{fb}) was calculated from the Mott-Schottky plots. To obtain the Mott-Schottky plot, the Ga-SnO₂-NC film was soaked in a 0.5M Na₂SO₄ aqueous solution and the impedance was measured as a function of the applied AC voltage (500 Hz, 10mV). The standard three-electrode configuration was used, with a platinum wire as the counter electrode and a Ag/AgCl electrode as the reference.

3. RESULTS AND DISCUSSION

Ga-doped SnO₂ nano-cuboids (Ga-SnO₂-NC) were hydrothermally grown using the commercial SnO₂-NPs as the seeds with the doping level controlled by the molar ratio between Ga and Sn precursors (1, 3, or 5%). Field emission scanning electron microscopy (FESEM) shows that the sizes of the SnO₂-NP range from 10-100 nm (Figure 1a). After hydrothermal deposition, aggregates of nano-cuboids (20-50 nm) are obtained (Figure 1b). Figure 1c and 1d shows high resolution transmission electron microscopy (HRTEM) reveals that the inter-planar

spacing of the nano-cuboid crystal is ~ 0.45 nm corresponding to the distance of the neighboring (100) planes in tetragonal rutile SnO_2 structure. The morphology of Ga- SnO_2 -NC is distinct to the previously reported Zn-doped SnO_2 .^{27, 28}

X-ray photoelectron spectroscopy (XPS) shows that Ga $2p_{2/3}$ peak (at 1117.1 eV) arises commensurate with the used dose of Ga precursor (Figure 2a), indicating the success of Ga doping. With 1% Ga precursor, the trace amount of Ga is not detectable by XPS. While the use of 3% (or 5%) Ga precursor gives the ratio of Ga to Sn to 0.024 (or 0.035) in the obtained Ga- SnO_2 -NCs. Consistently, the peaks of Sn $3d_{5/2}$ and Sn $3d_{3/2}$ in XPS spectrum left-shift with increasing Ga doping level resulting from the defects and charge imbalance induced by the dopants (Figure 2b).^{29, 30} The symmetric and narrow peaks ($\text{FWHM} \approx 1.35 \pm 0.05$ eV) suggest the oxidation state of Sn to be 4+.³¹⁻³³ On the other hand, Ga-doping does not alter the X-ray diffraction (XRD) spectrum of Ga- SnO_2 -NC (Figure 2c) which exhibits prominent diffraction angles at 26.6° , 33.9° and 51.8° , corresponding well to the rutile tetragonal SnO_2 (JCPDS, 41-1445). This suggests that the dopants are well-dispersed and do not cause significant change in the SnO_2 lattice structure. The sharp XRD peaks indicates that Ga- SnO_2 -NCs exhibit high crystallinity with the grain size of ~ 42.2 nm (similar to the size of nano-cuboid) which is estimated by Scherer's formula: $D = K\lambda/(\beta\cos\theta)$, where D is the grain size, K is Scherer constant (usually taken as 0.94) and β is the full-width-at-half-maximum (FWHM) for the peak centered at 0.464 radians.³⁴ Thus, individual nano-cuboids are essentially single crystals.

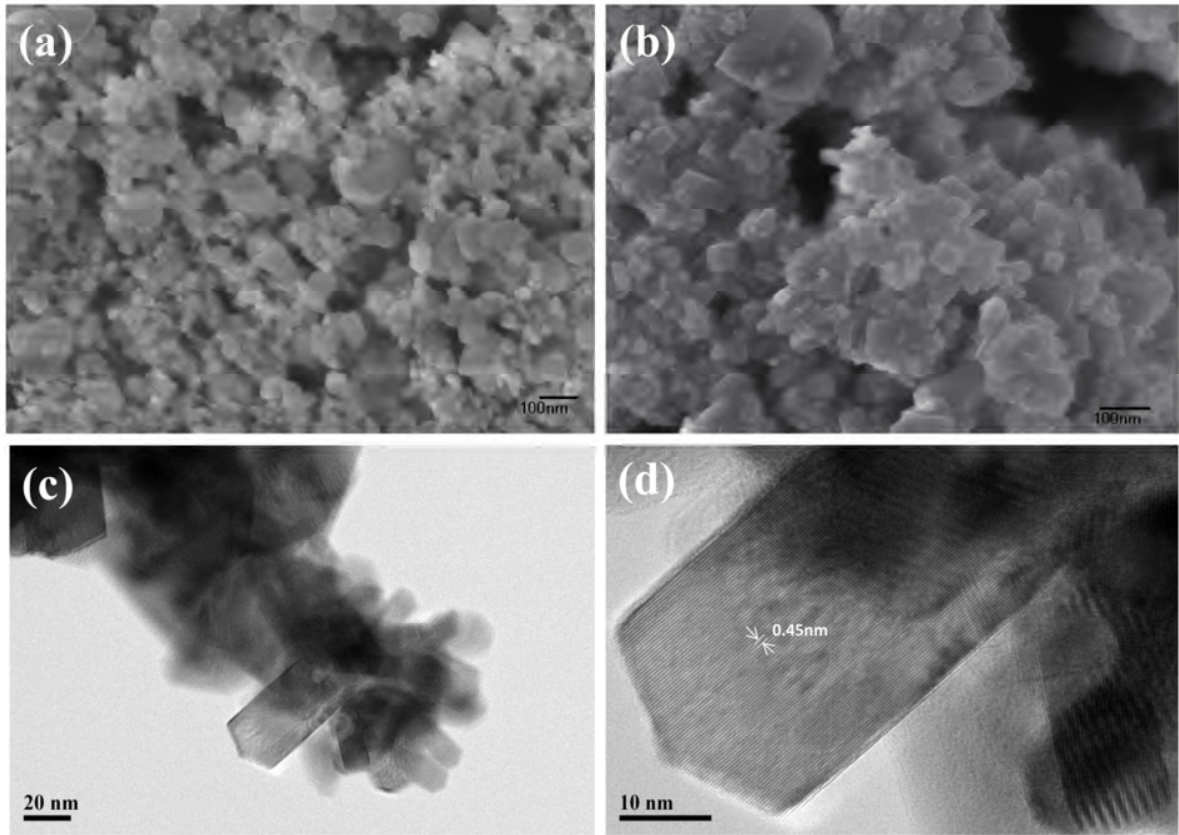


Figure 1. (a) FESEM image of SnO₂-NP, (b) FESEM image of Ga-SnO₂-NC, (c, d) HR-TEM of Ga-SnO₂-NC.

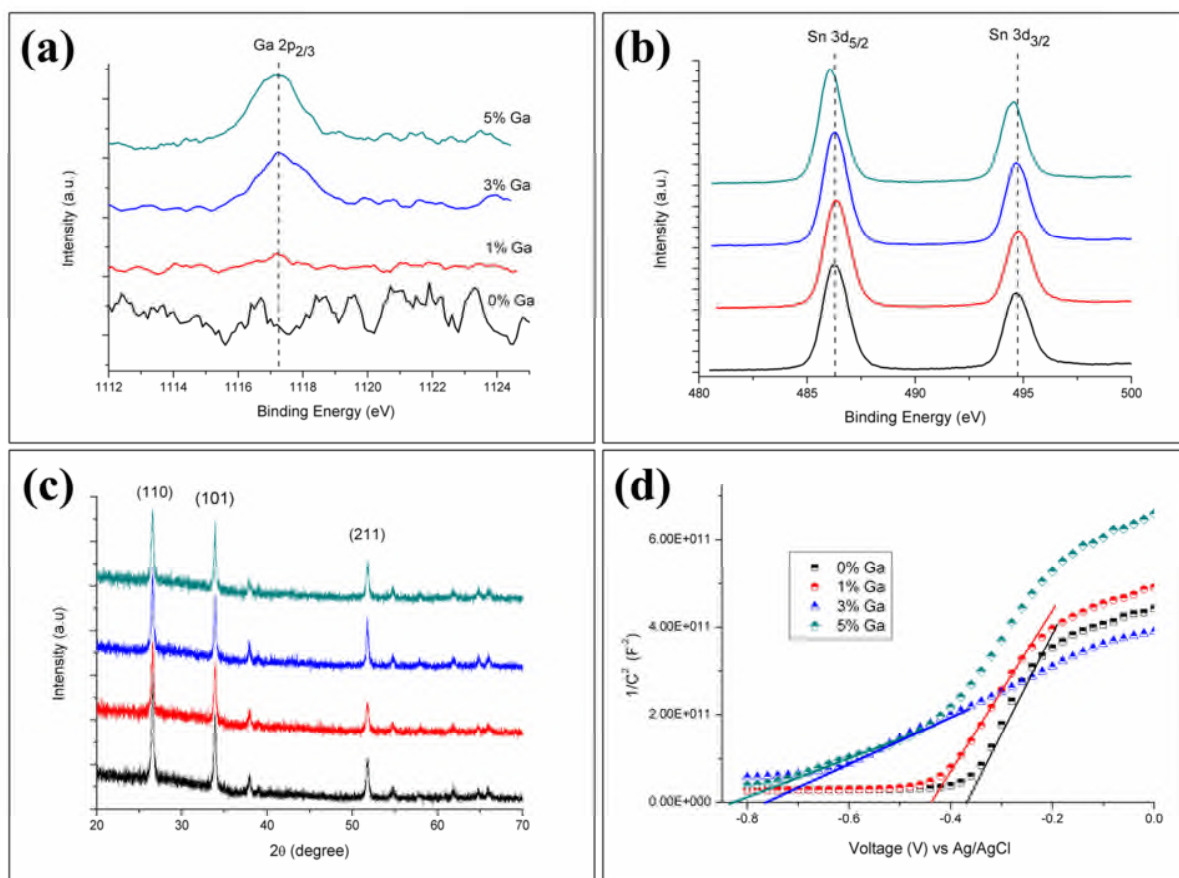


Figure 2. XPS spectra (a and b), XRD patterns (c), and Mott-Schottky plots of Ga-SnO₂-NCs with different doping levels (black, red, blue, green curves correspond to the use of 0, 1, 3, 5% of Ga-precursor during synthesis, respectively). In the y-axis of Mott-Schottky plot, C refers to interfacial capacitance.

The difference between the Fermi level of the active semiconducting material in a DSSC and the oxidation potential of the electrolyte determines the V_{oc} of DSSC. In order to ascertain the effect of Ga-doping towards the band edge or Fermi level, flat-band potentials (V_{fb}) of Ga-SnO₂-NC based photoanode were determined from Mott-Schottky plots (Figure 2d).³⁵⁻³⁷ According to the Mott-Schottky theory, $V_{fb} = E - kT/e$ where E is interpolated from the linear fitting of the

transition region of Mott-Schottky plots with x-axis; k is the Boltzman constant; T is the temperature; e is the elementary charge.³⁸ As shown in Figure 2d, V_{fb} left-shifts with increasing Ga-doping (from -0.34 with 0% Ga to -0.81 V with 5% Ga precursor), indicating that Ga-doping causes increase of Fermi-level which promises a higher V_{oc} and a higher fill-factor due to enhanced impedance to the backflow of photoelectrons to the electrolyte. UV-vis absorption measurements suggest that Ga-doping leads to up-shift of band edge instead of widening the band gap of SnO_2 (Figure S1 in Supporting Information).

To make the photoanode, the commercial SnO_2 -NPs or the prepared Ga- SnO_2 -NCs were doctor-bladed onto FTO substrate followed by immersion into a mixture of dye D149 and N719. Dye 149 adheres well with Ga- SnO_2 -NC whereas N719 absorbs short-wavelength light more efficiently (desirable for high V_{oc}).^{39, 40} Using D149 alone provides high short circuit current density (J_{sc}) but low open circuit voltage (V_{oc}) while using N719 alone does the opposite. We found that the ratio of 1:19 between D149 and N719 gives the highest power conversion efficiency due to the synergistic combination of the two dyes. This ratio is thus used for all the following experiments.

The fabricated DSSCs using a platinum counter electrode were then evaluated under the illumination of one sun condition (100 mW cm^{-2}). Figure 3a depicts the current density-voltage (J-V) curves of DSSCs equipped with SnO_2 -NP based anode or Ga- SnO_2 -NC based anodes. As shown in Table 1, a remarkable enhancement (61%) of power conversion efficiency (PCE) is observed with SnO_2 -NCs (without doping) as compared with SnO_2 -NPs despite that SnO_2 -NPs even has a higher dye loading capacity. The enhancement is attributable to the improved inter-connectivity between SnO_2 nano-cuboids as compared with that of SnO_2 nanoparticles. With Ga-doping (3% Ga precursor), PCE is further boosted by 124% to 4.05%. Higher Ga-doping (5%)

achieves high V_{oc} (0.75V) and fill factor (FF, 74.6%) due to elevation of band edge. These values outperform that of all previously reported SnO_2 based DSSCs without TiO_2 coating. It is, however, arguable that Ga-doping may increase the dye-loading capacity.²⁷ As shown in Table 1, doping only slightly increases the dye-loading which cannot account for the significant improvement of PCE. But, on the other hand, high-level of Ga-doping (5%) leads to decrease of J_{sc} because too high a band edge impedes injection of photoelectrons thereby degrades PCE.

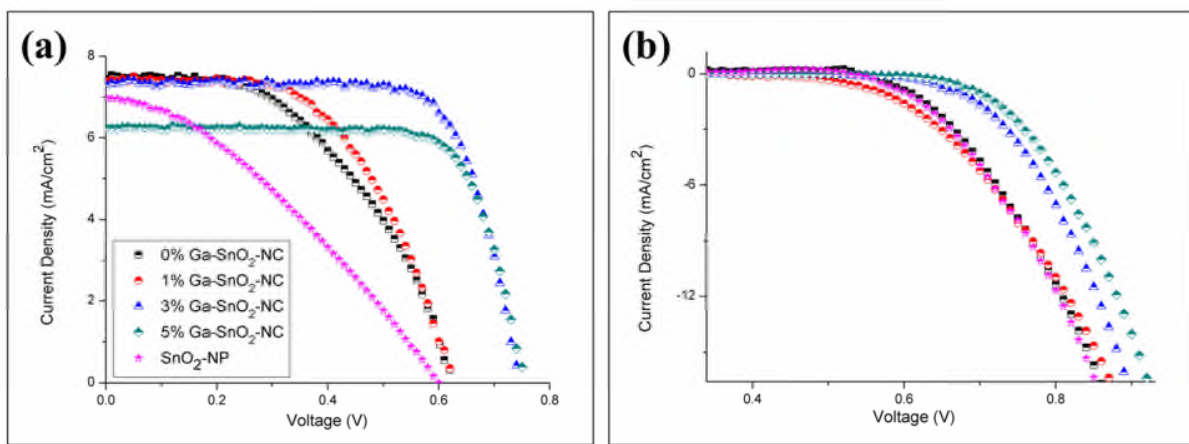


Figure 3. (a) Photocurrent density vs. voltage measured under the simulated sunlight (100 mW cm⁻²). (b) Dark currents of the DSSCs equipped with SnO_2 -NP or Ga-SnO_2 -NC based photoanode. Black, red, blue, green curves correspond to the use of 0, 1, 3, 5% of Ga-precursor during synthesis, respectively.

The dark current of a DSSC represents the backflow of electrons from the photoanode to the redox electrolyte and dye. Hence the higher onset potential to turn on the dark current suggests a lower charge recombination rate.^{41, 42} As observed from Figure 3b, DSSCs equipped with SnO_2 -NP, SnO_2 -NC, or slightly-doped Ga-SnO_2 -NC (1% Ga precursor) based photoanode exhibit similar charge recombination rate. Nevertheless the recombination rate decreases desirably when

Ga-SnO₂-NCs are doped to a higher level (3 or 5 % Ga precursor) because significantly elevated band edge leads to high resistance for electron back-flow to the electrolyte (Figure 4).

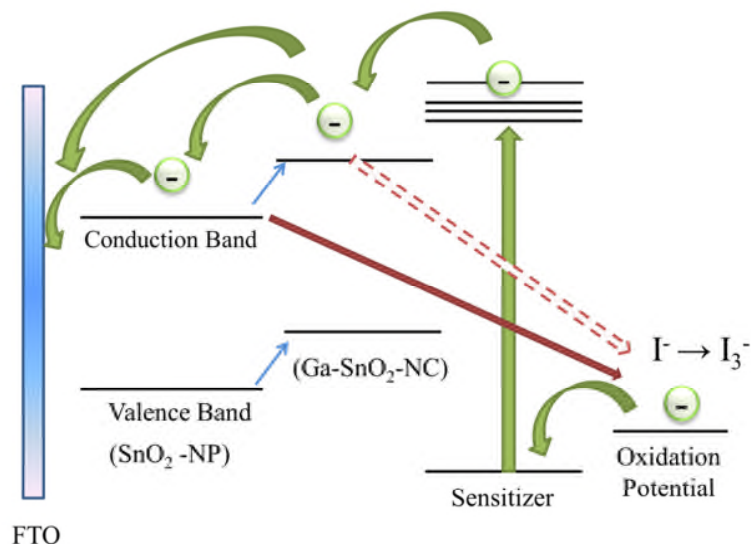


Figure 4 Illustration of band structures and electron transfers

Electrochemical impedance spectroscopy (EIS) was employed to further investigate the effect of Ga-doping on the charge transport and transfer properties of the DSSC. Figure 5 shows the Nyquist plots of DSSCs using SnO₂-NC photoanode with different Ga-doping levels, measured under 100mWcm⁻² light illumination, with frequencies ranging from 0.1 to 100 kHz and an alternating current amplitude of 10 mV. The curves are fitted with the equivalent circuit illustrated in the inset where R_s is the series resistance; R_a or R_{pt} represents the interfacial charge transfer resistances at the photoanode or counter electrode (the fitted parameters shown in table S1 in SI); CPE1 and CPE2 are the Helmholtz capacitance at respective electrodes.⁴³ In the Nyquist plot, the size of the smaller semicircle at high frequency range corresponds to the total charge transfer impedance at the counter electrode (R_{pt} in parallel with CPE2) while the larger semicircle at low frequency range corresponds to that of photoanode (R_a in parallel with CPE1).

The ease of electron transfer from excited sensitizer (dye) molecules to electrode and the difficulty of electron backflow to electrolyte lead to a small R_a .⁴⁴⁻⁴⁶ The EIS measurements reveal that R_a of photoanode largely drops from 89.3 to 53.9 Ω when Ga-doping increases to 3% (precursor concentration). This is because 1) Ga-SnO₂-NC, with an elevated conduction band approaching that of the sensitizer, serves as a bridge to facilitate electron transfer from the sensitizer to the underlying SnO₂-NP and subsequently the electrode or to the electrode directly; 2) increased difference between the elevated conduction band and the oxidation potential of the electrolyte also impedes the electron backflow to electrolyte (Figure 4). Reduced R_a leads to improved V_{oc} and FF (Table 1).

Table 1 Comparison of photovoltaic parameters for DSSCs with a SnO₂-NP or Ga-SnO₂-NC based photoanode. The percentage values indicate the concentration of Ga-precursor used in the synthesis.

Sample (n = 5)	Dye loading ($\times 10^8$ mol cm ⁻²)	V_{oc} (V)	J_{sc} (mA/cm ²)	$FF = \frac{P_{max}}{J_{sc}V_{oc}}$ (%)	$PCE = \frac{J_{sc}V_{oc}FF}{P_{in}}$ (%)
SnO₂-NP	8.94 \pm 0.30	0.59 \pm 0.017	7.00 \pm 0.110	34.4 \pm 4.14	1.42 \pm 0.326
0% Ga-SnO₂-NC	7.02 \pm 0.43	0.62 \pm 0.000	7.56 \pm 0.176	48.9 \pm 2.42	2.29 \pm 0.120
1% Ga-SnO₂-NC	7.22 \pm 0.27	0.62 \pm 0.006	7.51 \pm 0.350	55.6 \pm 1.40	2.59 \pm 0.068
3% Ga-SnO₂-NC	7.58 \pm 0.55	0.74 \pm 0.012	7.41 \pm 0.085	73.7 \pm 1.10	4.05 \pm 0.135
5% Ga-SnO₂-NC	7.66 \pm 0.13	0.75 \pm 0.006	6.30 \pm 0.143	74.6 \pm 0.57	3.52 \pm 0.070

However, further doping (5% Ga-precursor) causes increase of R_a because an over-boosted conduction band of Ga-SnO₂-NC (greater than that of sensitizer) by a high doping level increases electron injection resistance. This explains the observed reduction in short-circuit current (J_{sc}) at this doping level (Table 1). Therefore, doping with 3% Ga-precursor is optimal to achieve high PCE.

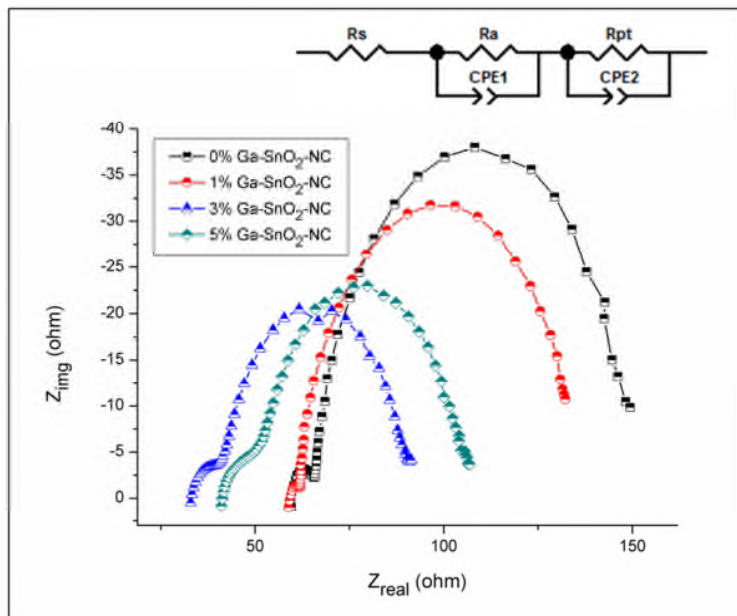


Figure 5. Nyquist plots of DSSCs equipped with a Ga-SnO₂-NC based photoanode. The percentage values indicate the concentration of Ga-precursor used in synthesis. Inset shows the equivalent circuit.

To further confirm that gallium doping has indeed suppressed charge recombination, open-circuit voltage-decay (OCVD) technique was employed in which the decrease in V_{oc} is continuously monitored while turning off the light shone on the device (Figure 6a). The electron lifetime is then calculated using the formula: $\tau_n = -(kT/e)(dV_{oc}/dt)^{-1}$, where kT is the thermal energy; e is the positive elementary charge; and dV_{oc}/dt is the decaying rate of V_{oc} .⁴⁷ As shown in Figure 6b,

SnO₂-NP has the shortest electron lifetime, and the electron lifetime is significantly increased at high doping level (5%). The increase of electron lifetime implies lower charge recombination from the mesoporous oxide towards the electrolyte.

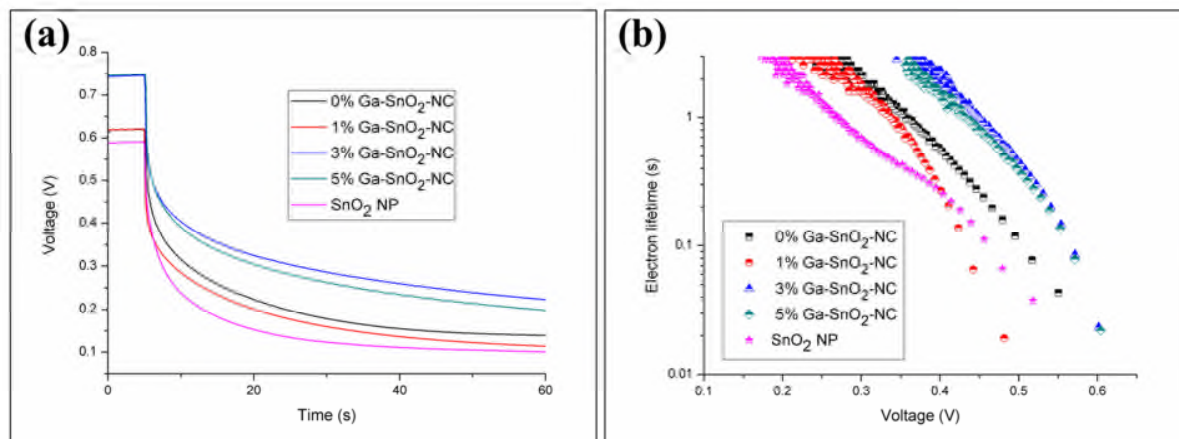


Figure 6. (a) Open-circuit voltage-decay (OCVD) curves and (b) electron lifetime as a function of V_{oc} for DSSCs equipped with SnO₂-NP or Ga-SnO₂-NC based photoanode.

CONCLUSION

In summary, we have demonstrated a DSSC with a Ga-SnO₂-NC photoanode, which achieves high open-circuit potential, fill-factor, and photo conversion efficiency. The improved performance is resulted from moderate up-shift of the band edge by Ga-doping which increases open circuit voltage, facilitates electron injection from the sensitizer to the electrode, and impedes electron recombination with the electrolyte. This study shows that the performance of SnO₂-based DSSCs can be improved by engineering the band structure of SnO₂.

ASSOCIATED CONTENT

Supporting Information

Optical band gap of Ga-SnO₂-NC.

This material is available free of charge via the Internet at <http://pubs.acs.org>.

AUTHOR INFORMATION

Corresponding Author

*Correspondence to: chenpeng@ntu.edu.sg

Notes

The authors declare no competing financial interest.

ACKNOWLEDGEMENT

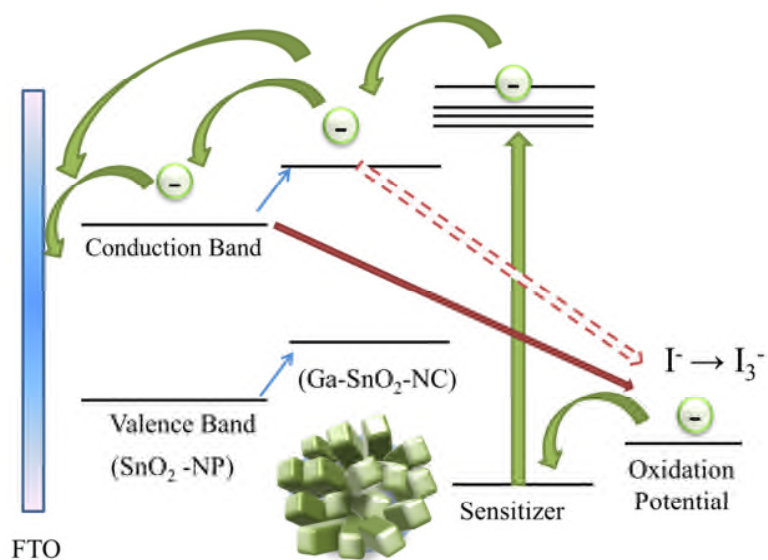
This work is financially supported by the Agency for Science, Technology and Research (A*STAR) under SERC Grant No. 102 170 0142. We also thank GlobalFoundries (Singapore) for the scholarship provided to J.J. Teh and S.L. Ting.

REFERENCES

1. Guai, G.H.;Leiw, M.Y.;Ng, C.M.;Li, C.M., *Adv. Energy Mater.* **2012**, 2, 334-338.
2. Guai, G.H.;Li, Y.;Ng, C.M.;Li, C.M.;Chan-Park, M.B., *ChemPhysChem.* **2012**, 13, 2566-2572.
3. O'Regan, B.Gratzel, M., *Nature* **1991**, 353, 737-740.
4. Wang, W.;Zhao, Q.;Li, H.;Wu, H.;Zou, D.;Yu, D., *Adv. Funct. Mater.* **2012**, 22, 2775-2782.
5. Yella, A.;Lee, H.-W.;Tsao, H.N.;Yi, C.;Chandiran, A.K.;Nazeeruddin, M.K.;Diau, E.W.-G.;Yeh, C.-Y.;Zakeeruddin, S.M.;Grätzel, M., *Science* **2011**, 334, 629-634.
6. Greijer Agrell, H.;Lindgren, J.;Hagfeldt, A., *Sol. Energy* **2003**, 75, 169-180.
7. Arnold, M.S.;Avouris, P.;Pan, Z.W.;Wang, Z.L., *J. Phys. Chem. B* **2002**, 107, 659-663.
8. Teh, J.J.;Guai, G.H.;Wang, X.;Leong, K.C.;Li, C.M.;Chen, P., *J. Renewable Sustainable Energy* **2013**, 5, 023120-8.
9. Green, A.N.M.;Palomares, E.;Haque, S.A.;Kroon, J.M.;Durrant, J.R., *J. Phys. Chem. B* **2005**, 109, 12525-12533.
10. Chappel, S.Zaban, A., *Sol. Energy Mater. Sol. Cells* **2002**, 71, 141-152.
11. Fukai, Y.;Kondo, Y.;Mori, S.;Suzuki, E., *Electrochem. Commun.* **2007**, 9, 1439-1443.
12. Nang Dinh, N.;Bernard, M.-C.;Hugot-Le Goff, A.;Stergiopoulos, T.;Falaras, P., *C. R. Chim.* **2006**, 9, 676-683.
13. Zhu, K.;Neale, N.R.;Miedaner, A.;Frank, A.J., *Nano Lett.* **2006**, 7, 69-74.
14. Ramasamy, E.Lee, J., *J. Phys. Chem. C* **2010**, 114, 22032-22037.
15. Park, N.G.;Kang, M.G.;Kim, K.M.;Ryu, K.S.;Chang, S.H.;Kim, D.K.;van de Lagemaat, J.;Benkstein, K.D.;Frank, A.J., *Langmuir* **2004**, 20, 4246-4253.
16. Kim, M.-H.Kwon, Y.-U., *J. Phys. Chem. C* **2009**, 113, 17176-17182.
17. Kim, M.-H.Kwon, Y.-U., *J. Phys. Chem. C* **2011**, 115, 23120-23125.
18. Pang, H.;Yang, H.;Guo, C.X.;Li, C.M., *ACS Appl. Mater. Interfaces* **2012**, 4, 6261-6265.
19. Shang, G.;Wu, J.;Tang, S.;Liu, L.;Zhang, X., *J. Phys. Chem. C* **2013**, 117, 4345-4350.
20. Kim, D.W.;Shin, S.S.;Cho, I.S.;Lee, S.;Kim, D.H.;Lee, C.W.;Jung, H.S.;Hong, K.S., *Nanoscale* **2012**, 4, 557-562.
21. Chen, J.;Lu, L.;Wang, W., *J. Phys. Chem. C* **2012**, 116, 10841-10847.
22. Li, Z.;Zhou, Y.;Bao, C.;Xue, G.;Zhang, J.;Liu, J.;Yu, T.;Zou, Z., *Nanoscale* **2012**, 4, 3490-3494.
23. Li, Y.;Wang, Y.;Chen, C.;Pang, A.;Wei, M., *Chem. Eur. J.* **2012**, 18, 11716-11722.
24. Zhang, Y.;Zhang, H.;Wang, Y.;Zhang, W.F., *J. Phys. Chem. C* **2008**, 112, 8553-8557.
25. Shin, S.S.;Kim, J.S.;Suk, J.H.;Lee, K.D.;Kim, D.W.;Park, J.H.;Cho, I.S.;Hong, K.S.;Kim, J.Y., *ACS Nano* **2013**, 7, 1027-1035.
26. Ito, S.;Chen, P.;Comte, P.;Nazeeruddin, M.K.;Liska, P.;Péchy, P.;Grätzel, M., *Prog. Photovoltaics* **2007**, 15, 603-612.
27. Ramasamy, E.Lee, J., *Energy Environ. Sci.* **2011**, 4, 2529-2536.
28. Dou, X.;Sabba, D.;Mathews, N.;Wong, L.H.;Lam, Y.M.;Mhaisalkar, S., *Chem. Mater.* **2011**, 23, 3938-3945.
29. Dobler, D.;Oswald, S.;Wetzig, K., *Anal. Bioanal. Chem.* **2002**, 374, 646-649.
30. Yang, J.;Hidajat, K.;Kawi, S., *J. Mater. Chem.* **2009**, 19, 292-298.
31. Chang, S.T.;Leu, I.C.;Hon, M.H., *J. Cryst. Growth* **2004**, 273, 195-202.
32. Sun, S.;Meng, G.;Zhang, G.;Masse, J.-P.;Zhang, L., *Chem. Eur. J.* **2007**, 13, 9087-9092.
33. Szuber, J.;Czempik, G.;Larciprete, R.;Koziej, D.;Adamowicz, B., *Thin Solid Films* **2001**, 391, 198-203.

34. Azároff, L.V., *Elements of X-ray crystallography*; McGraw-Hill: New York, **1968**, pp. 552
35. Radecka, M.;Rekas, M.;Trenczek-Zajac, A.;Zakrzewska, K., *J. Power Sources* **2008**, 181, 46-55.
36. Bandara, J.Pradeep, U.W., *Thin Solid Films* **2008**, 517, 952-956.
37. Parks, G.A., *Chem. Rev.* **1965**, 65, 177-198.
38. Xiang, P.;Li, X.;Wang, H.;Liu, G.;Shu, T.;Zhou, Z.;Ku, Z.;Rong, Y.;Xu, M.;Liu, L.;Hu, M.;Yang, Y.;Chen, W.;Liu, T.;Zhang, M.;Han, H., *Nanoscale Res. Lett.* **2011**, 6, 606.
39. Onwona-Agyeman, B.K., Shoji; Kumara, Asoka; Okuya, Masayuki; Murakami, Kenji; Konno, Akinori; Tennakone, Kirthi, *Jpn. J. Appl. Phys.* **2005**, 44, 731.
40. Ariyasinghe, Y.P.Y.P.;Wijayarathna, T.R.C.K.;Kumara, I.G.C.K.;Jayarathna, I.P.L.;Thotawatthage, C.A.;Gunathilake, W.S.S.;Senadeera, G.K.R.;Perera, V.P.S., *J. Photochem. Photobiol., A* **2011**, 217, 249-252.
41. O'Regan, B.C.;López-Duarte, I.;Martínez-Díaz, M.V.;Forneli, A.;Albero, J.;Morandeira, A.;Palomares, E.;Torres, T.;Durrant, J.R., *J. Am. Chem. Soc.* **2008**, 130, 2906-2907.
42. Splan, K.E.;Massari, A.M.;Hupp, J.T., *J. Phys. Chem. B* **2004**, 108, 4111-4115.
43. Lee, S.;Noh, J.H.;Han, H.S.;Yim, D.K.;Kim, D.H.;Lee, J.-K.;Kim, J.Y.;Jung, H.S.;Hong, K.S., *J. Phys. Chem. C* **2009**, 113, 6878-6882.
44. Fuke, N.;Fukui, A.;Komiya, R.;Islam, A.;Chiba, Y.;Yanagida, M.;Yamanaka, R.;Han, L., *Chem. Mat.* **2008**, 20, 4974-4979.
45. Papageorgiou, N.;Maier, W.F.;Grätzel, M., *J. Electrochem. Soc.* **1997**, 144, 876-884.
46. Wang, Q.;Moser, J.-E.;Grätzel, M., *J. Phys. Chem. B* **2005**, 109, 14945-14953.
47. Archana, P.S.;Jose, R.;Vijila, C.;Ramakrishna, S., *J. Phys. Chem. C* **2009**, 113, 21538-21542.

Graphic Abstract



We demonstrate an improved dye-sensitized solar cell equipped with a photoelectrode based on gallium-doped SnO₂ nano-cuboids.